Structural, Thermal, Optical, Luminescence and Dielectric Studies of Nd^{3+}-Doped Lithium Borate Glasses Prepared by the Melt-Quenching Technique

T Firoz khan[1], J Chandra Sekhar [2], D Chandra Sekhar[3], Sake Devendra[4] , Pavani Suggana[5]
[1,3,4,5] *Government College Autonomous, Anantapur, A.P, India*
[2]*SCNR Government Degree College, Proddatur, YSR Kadapa, A.P, India*
doi.org/10.64643/IJIRTV13I4-208628-459

***Abstract*—Rare-earth-ion-incorporated borate glasses have attracted considerable attention as advanced optical materials owing to their superior optical transparency, high chemical resistance, excellent thermal stability, and remarkable luminescence performance. In the present study, the composition of 69 mol% B_2O_3–30 mol% LiF–1 mol% Nd_2O_3 lithium borate glass was successfully synthesized via the conventional melt-quenching method. The undoped glass of composition 70 mol% B_2O_3–30 mol% LiF was served as the reference matrix. A comprehensive characterization of the prepared glasses was carried out through X-ray diffraction (XRD), Fourier Transform Infrared (FTIR) spectroscopy, Raman spectroscopy, thermogravimetric–differential thermal analysis (TG–DTA), UV–Visible–NIR absorption spectroscopy, photoluminescence spectroscopy, and dielectric measurements to evaluate their structural, thermal, optical, and electrical properties.**

The non-crystalline nature of both glass samples was verified by the results of X-Ray Diffraction Spectra, whereas the formation of a borate glass network composed predominantly of BO_3 and BO_4 structural units were confirmed by FTIR and Raman spectra. Thermal studies indicated favourable glass stability with a well-defined glass transition temperature and characteristic crystallization behaviour. The optical absorption spectra displayed the characteristic electronic transitions associated with Nd^{3+} ions. Further, strong near-IR emission bands centred at approximately 894, 1063, and 1330 nm were observed, corresponding to the $^4F_{3/2} \rightarrow {}^4I_{9/2}$, $^4I_{11/2}$, and $^4I_{13/2}$ transitions, respectively. Dielectric measurements exhibited the typical frequency-dependent dielectric dispersion accompanied by a progressive increase in AC conductivity with increasing frequency. Overall, the results confirm that Nd^{3+}-doped lithium borate glass owns excellent structural stability, high optical quality, and efficient luminescent behaviour, highlighting its potential for applications such as solid-state laser systems, optical amplifiers, photonic technologies, and optical fiber communication.

***Index Terms*—X-ray diffraction (XRD), Fourier Transform Infrared (FTIR) Spectroscopy, Raman Spectroscopy, Thermo Gravimetric–Differential Thermal Analysis (TG–DTA), UV–Visible Spectroscopy**

I. INTRODUCTION

Glass is an amorphous, non-crystalline solid that forms through a glass-transition process, during which a viscous liquid is transformed into a rigid solid without the development of long-range structural order. In contrast to crystalline materials, glasses lack periodic atomic arrangement while retaining isotropic physical and optical characteristics. Their high optical transparency, compositional flexibility, ease of processing, and relatively low manufacturing cost make them versatile materials for advanced technological applications. Therefore, glasses have attracted considerable interest for use in optical-fiber systems, laser-host media, display technologies, optical and chemical sensors, and a wide range of optoelectronic devices.

Among the various glass-forming systems, borate-based glasses have attracted significant research interest owing to their relatively low melting temperature, high capacity for rare-earth-ion incorporation, excellent optical transparency, and versatile optical characteristics. The introduction of rare-earth ions, particularly Nd^{3+}, imparts distinctive

spectroscopic features associated with electronic transitions within the partially filled 4f electronic configuration. These characteristics make rare-earth-doped borate glasses promising host materials for a broad range of photonic and optoelectronic applications.

Among the rare-earth activators, Nd^{3+} ions are widely recognized as efficient laser-active centres because of their strong absorption and emission transitions spanning the visible and near-infrared spectral regions [1-3]. Therefore, Nd^{3+}-doped lithium borate glasses are attractive candidates for applications such as solid-state lasers, optical amplifiers, fiber-optic communication systems, and other communication devices (4-6).

II. EXPERIMENTAL PROCEDURE

Reference and Nd^{3+}-doped lithium borate glasses were prepared using the conventional melt-quenching technique. Two glass compositions were investigated: a reference glass containing 70 mol% B_2O_3 and 30 mol% LiF, and an Nd^{3+}-doped composition consisting of 69 mol% B_2O_3, 30 mol% LiF, and 1 mol% Nd_2O_3, as summarized in Table 1[7-9]

Sample	Composition (mol%)
Reference glass	70 B_2O_3–30 LiF
Nd^{3+}-doped glass	69 B_2O_3–30 LiF–1 Nd_2O_3

Analytical-grade, high-purity starting materials were accurately weighed according to the stoichiometric ratio and thoroughly homogenized to ensure uniform distribution of the constituent components. The resulting batches were transferred to suitable crucibles and melted at 950 °C for 2 hours to promote complete melting and the homogeneous melts were subsequently rapidly quenched between preheated brass plates to suppress crystallization so as to form an amorphous glassy phase. The quenched samples obtained were transparent, circular discs with typical dimensions of approximately 1–2 cm in diameter and 0.3 cm in thickness. The prepared glasses were subsequently used for structural, thermal, optical, and spectroscopic characterization.

III. CHARACTERIZATION TECHNIQUES

The prepared glasses were characterized using:

- X-ray Diffraction (XRD)
- Fourier Transform Infrared Spectroscopy (FTIR)
- TG-DTA thermal analysis
- UV–Visible–NIR absorption spectroscopy
- Raman spectroscopy
- Near-infrared photoluminescence spectroscopy
- Dielectric measurements

These techniques provided information regarding structural, thermal, optical, vibrational and electrical properties.

IV. RESULTS AND DISCUSSION

4.1 XRD ANALYSIS OF $70B_2O_3$–30LiF GLASS

The structural nature of the prepared 70 mol% B_2O_3–30 mol% LiF glass was investigated by powder X-ray diffraction (XRD) over the 2θ range of 10–70°. The diffraction profile exhibits a broad and diffuse scattering pattern without distinct sharp Bragg reflections, confirming the predominantly amorphous nature of the prepared material. The absence of well-defined crystalline peaks indicates that long-range periodic atomic ordering is not present in the glass network and demonstrates successful glass formation after rapid quenching.

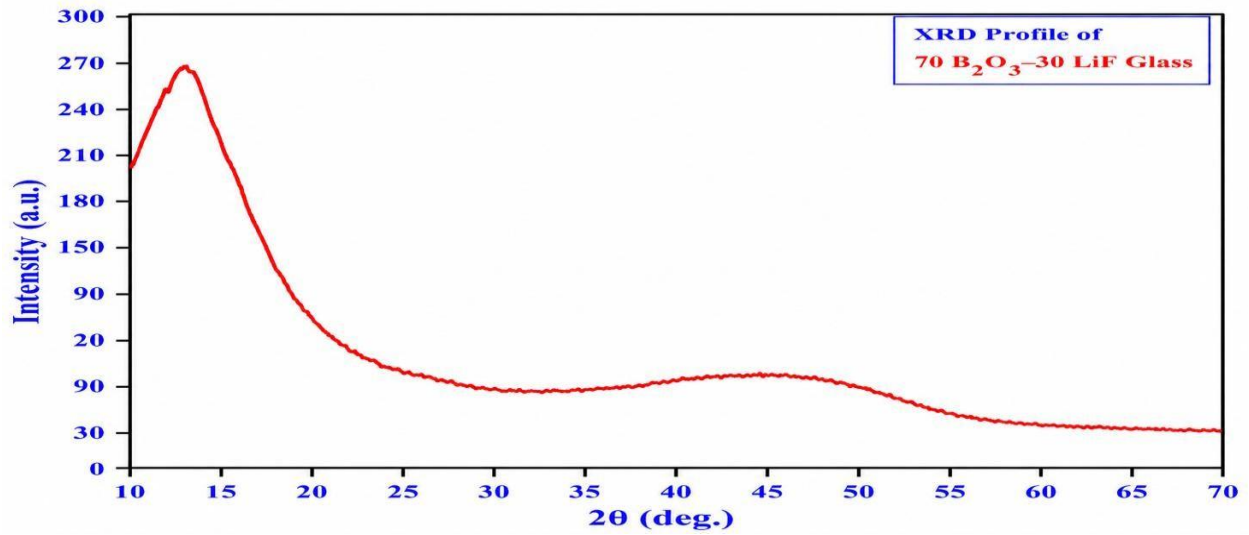

Fig.1: X-ray diffraction pattern of the 70 mol% B_2O_3–30 mol% LiF glass

A broad intensity distribution is observed in the low-angle region, followed by a gradual decrease in intensity and a weak diffuse hump extending approximately through the intermediate-angle region. Such broad features are characteristic of the short- and intermediate-range structural correlations associated with borate-based glass networks. The lack of narrow diffraction peaks further suggests that the melt-quenching process effectively suppressed crystallization during rapid cooling.

The observed amorphous structure can be attributed to the random arrangement of BO_3 and BO_4 structural units within the borate network, with LiF acting as a modifying component that influences the connectivity and local structural environment of the glass. Overall, the XRD results confirm the successful formation of a non-crystalline $70B_2O_3$–30LiF glass matrix, providing a suitable host for subsequent incorporation of rare-earth ions such as Nd^{3+}.

4.2 OPTICAL ABSORPTION

The host glass showed high ultraviolet transparency extending to approximately 350 nm. After Nd^{3+} incorporation, several sharp absorption bands appeared at approximately 351, 358, 431, 460, 474, 525, 583, 625, 683, 749, 803 and 877 nm. These sharp bands arise from electronic transitions within the partially filled 4f shell of Nd^{3+} ions.

The figure shows the optical absorption spectrum of Nd^{3+}-doped B_2O_3–LiF glass recorded in the wavelength range of approximately 300–1000 nm[10].

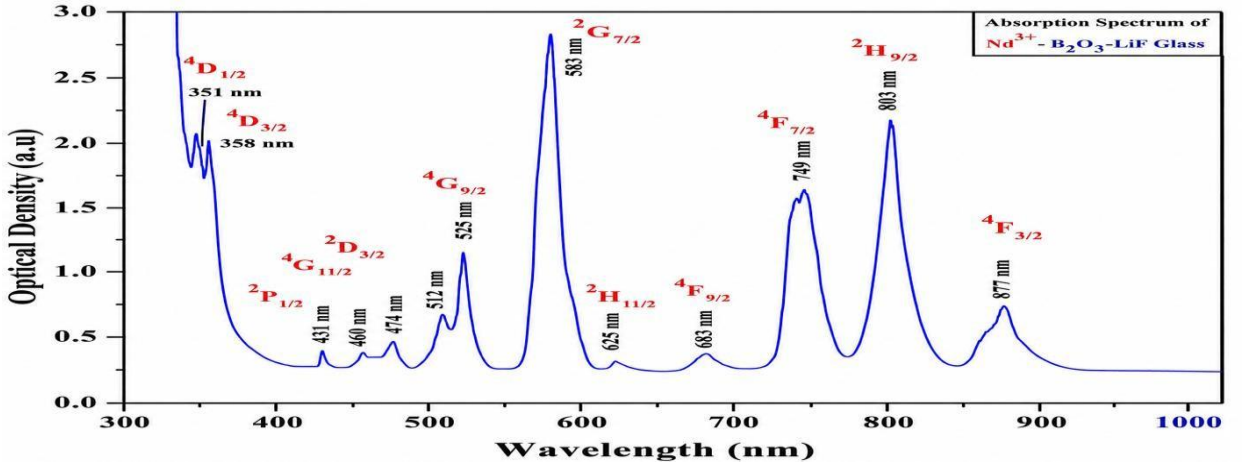

Fig.2: Absorption spectrum of Nd^{3+}:B_2O_3-LiF glass

- The strong bands in the UV region (≈350–525 nm) are attributed to transitions from the Nd^{3+} ground state $^4I_{9/2}$ to higher excited 4f energy levels.
- The prominent absorption around 583 nm corresponds to an Nd^{3+} electronic transition and shows relatively high optical absorption.
- The absorption band near 749 nm is comparatively strong and is associated with a transition to an excited Nd^{3+} level.
- The absorption around 877 nm is also characteristic of Nd^{3+} ions and occurs in the near-infrared region.
- The sharpness of the absorption bands indicates that the 4f electronic transitions of Nd^{3+} are relatively well defined and are only weakly affected by the glass network.
- The broad glass matrix provides the host environment, while the observed sharp bands originate mainly from Nd^{3+} ions.

The presence of several well-defined Nd^{3+} absorption bands confirms the successful incorporation of Nd^{3+} ions into the B_2O_3–LiF glass matrix [11]. The strong UV–visible and near-infrared absorption transitions demonstrate that the glass has potential for optical amplification, laser materials, fiber-optic devices, and photonic applications.

4.3 NIR EMISSION SPECTRUM: PHOTOLUMINESCENCE PROPERTIES

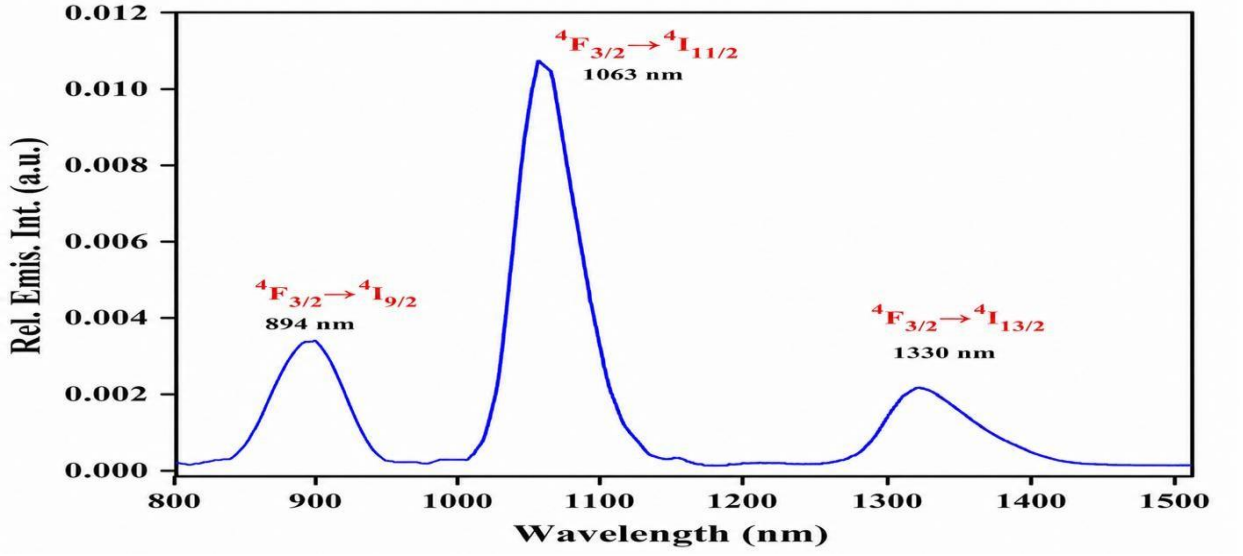

Fig.3: NIR emission spectrum of Nd^{3+}:B_2O_3-LiF glass with Ar^+ laser (514.5nm) as the pump source

From the NIR emission spectrum of Nd^{3+}:B_2O_3-LiF glass, three characteristic emission bands are clearly observed (11- 14):

Emission wavelength	Electronic transition	Relative intensity	Assignment
894 nm	$^4F_{3/2} \rightarrow {}^4I_{9/2}$	Moderate	NIR emission
1063 nm	$^4F_{3/2} \rightarrow {}^4I_{11/2}$	Highest	Dominant NIR emission
1330 nm	$^4F_{3/2} \rightarrow {}^4I_{13/2}$	Lower	NIR emission

These three bands are characteristic of Nd^{3+} ions. Nd^{3+} commonly exhibits emissions around 900, 1060 and 1330 nm arising from the $^4F_{3/2}$ excited state to the $^4I_{9/2}$, $^4I_{11/2}$ and $^4I_{13/2}$ levels, respectively. The spectrum therefore confirms the presence of Nd^{3+}-related NIR luminescence. All three observed transitions originate from the common excited $^4F_{3/2}$ level, followed by radiative relaxation to different lower-lying ^4I levels:

The 1063 nm emission is the strongest, demonstrating that the $^4F_{3/2} \rightarrow {}^4I_{11/2}$ transition is the dominant radiative pathway in the investigated sample. The presence of multiple NIR emission bands indicates that the material has promising photoluminescence and NIR optical properties, with possible relevance to solid-state lasers, optical

amplifiers, photonic devices and NIR imaging/sensing applications.

4.3 FTIR- ANALYSIS

The FTIR spectrum reveals a broad and intense absorption band centered at 3436 cm^{-1}, which is attributed to the stretching vibration of hydroxyl (–OH) groups originating from adsorbed water molecules or surface hydroxyl groups. Two weak absorption bands at 2924 cm^{-1} and 2854 cm^{-1} correspond to the asymmetric and symmetric stretching vibrations of aliphatic C–H bonds, indicating the presence of trace organic residues or precursor molecules. A medium-intensity band observed at 1634 cm^{-1} is assigned to the bending vibration of adsorbed H–O–H molecules and may also contain contributions from carbonyl (C=O) stretching.

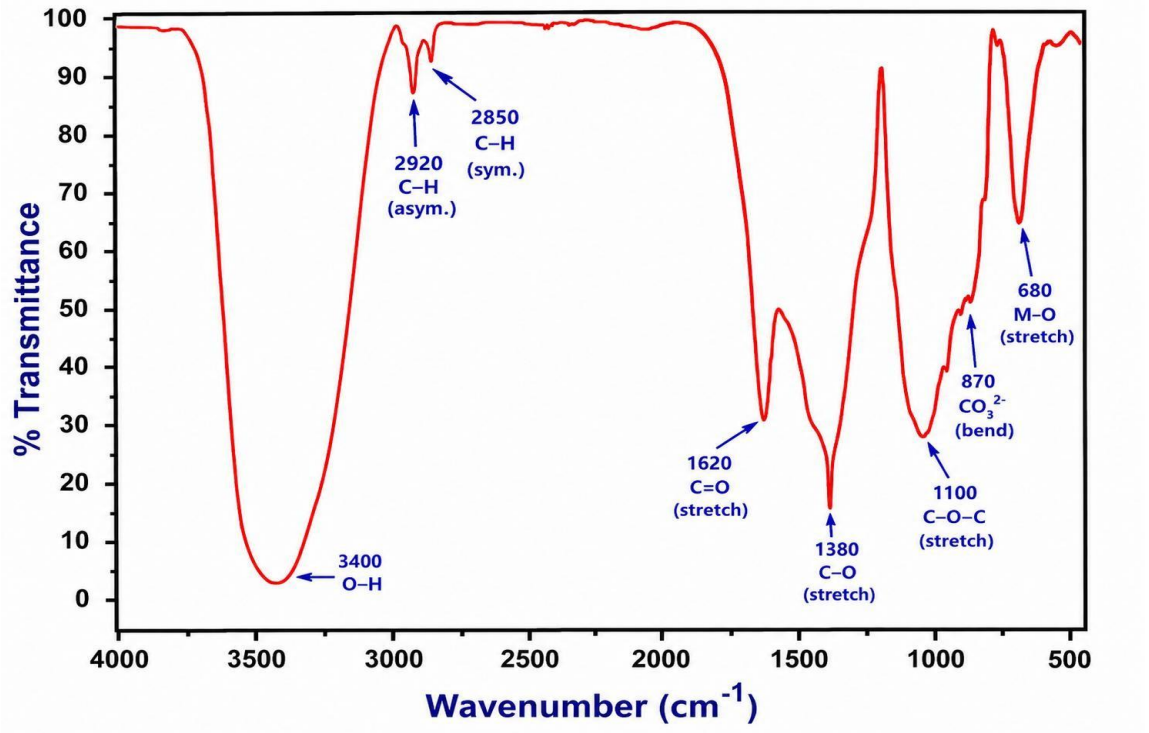

Fig.4: FTIR Spectrum of reference glass (B_2O_3-LiF)

A strong absorption band appearing at 1046 cm^{-1} corresponds to C–O/C–O–C stretching vibrations, confirming the presence of oxygen-containing functional groups. The characteristic low-wavenumber band at approximately 692 cm^{-1} is attributed to metal–oxygen (M–O) lattice vibrations, indicating successful formation of the inorganic metal oxide framework.

The FTIR analysis confirms the presence of hydroxyl groups, minor organic residues, oxygen-containing functional groups, and characteristic metal–oxygen bonds. The strong absorption observed below 700 cm^{-1} verifies the formation of the inorganic lattice, while the absence of numerous impurity bands suggests relatively high phase purity. The FTIR spectrum confirmed the formation of the borate glass network. Characteristic bands include

- 1375 cm^{-1} – BO_3 stretching vibration
- 1050 cm^{-1} – BO_4 tetrahedral units
- 750 cm^{-1} – B–O–B bending vibration
- 500 cm^{-1} – low-frequency vibration
- 3445 cm^{-1} – hydroxyl (OH) stretching

These observations indicate the coexistence of BO_3 and BO_4 structural units, which are responsible for the stability of the borate glass network.

4.5 THERMAL ANALYSIS

The thermal behaviour of the Nd^{3+}-doped B_2O_3–LiF glass sample was investigated using simultaneous Thermogravimetric Analysis (TGA) and Differential Scanning Calorimetry (DSC). The experiment was

carried out using a 13.887 mg sample over the temperature range of 30–1000 °C under a continuous heating programme.

Results and Discussion

The TGA curve indicates a multi-stage thermal decomposition process. In the initial stage (30–100 °C), a small weight loss of about 1.22% was observed, which can be associated with the removal of physically adsorbed moisture and volatile surface species.

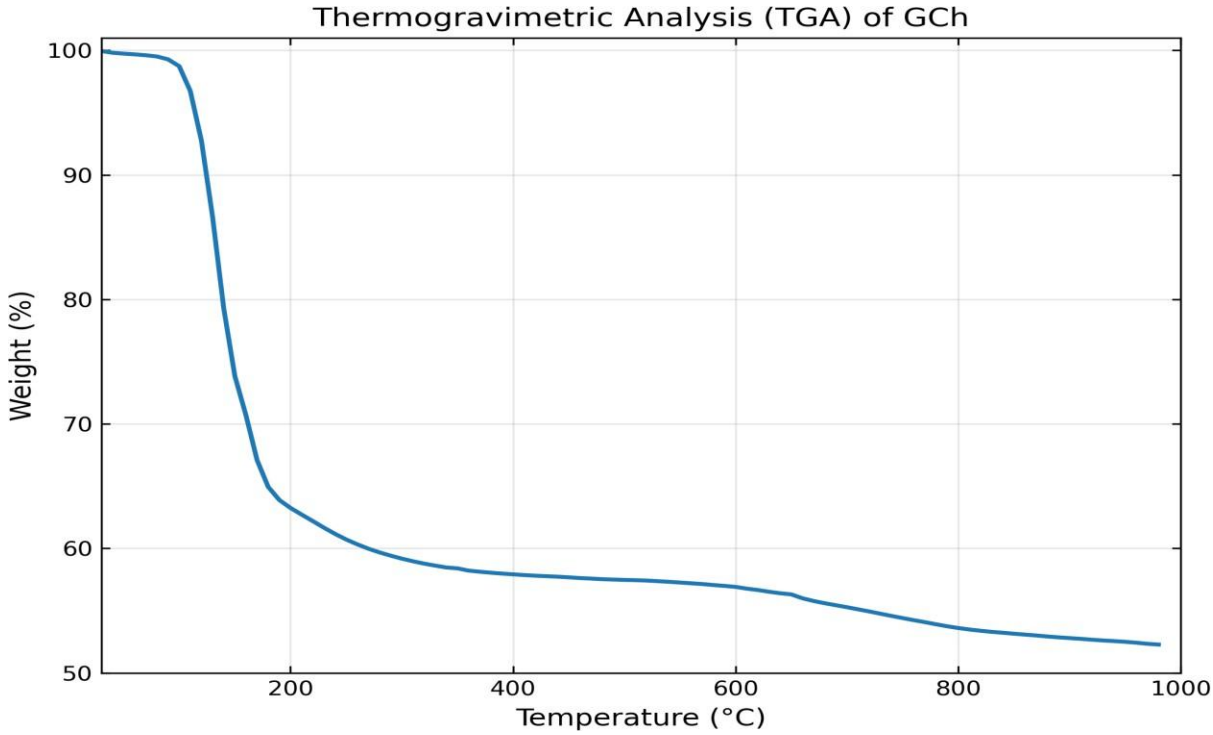

Fig.5: TGA curve (Weight % vs Temperature)

The major degradation occurred between 100 and 180 °C, where the sample lost approximately 33.79% of its mass. This represents the principal decomposition stage and is associated with the breakdown of organic constituents and other thermally labile groups. The maximum degradation rate occurred around 130–140 °C. Between 180 and 350 °C, a further weight loss of approximately 6.54% was observed, corresponding to continued decomposition, carbonization, and release of volatile gaseous products. Above 350 °C, the mass loss became considerably smaller, indicating the development of a comparatively stable residue.

The DSC results support the TGA observations. A broad endothermic event around 150 °C corresponds to moisture removal and major decomposition. An exothermic event around 380 °C is associated with structural rearrangement, carbonization, oxidation, or crystallization-related processes.

The sample exhibited an overall weight loss of approximately 47.67%, leaving a residual mass of about 52.28% at 980 °C. The relatively high residual mass and the slow mass loss at higher temperatures indicate the formation of a thermally stable carbonaceous and/or inorganic residue [15, 16].

The DSC–TGA investigation confirms that the Nd^{3+}:B_2O_3-LiF glass sample undergoes a well-defined, multi-stage thermal decomposition process. The principal degradation takes place between 100 and 180 °C, while the decomposition rate decreases substantially at higher temperatures. The residual mass of approximately 52.28% at 980 °C demonstrates significant thermal stability. Overall, the results indicate that the material possesses good resistance to high-temperature degradation and may be suitable for applications requiring enhanced thermal stability.

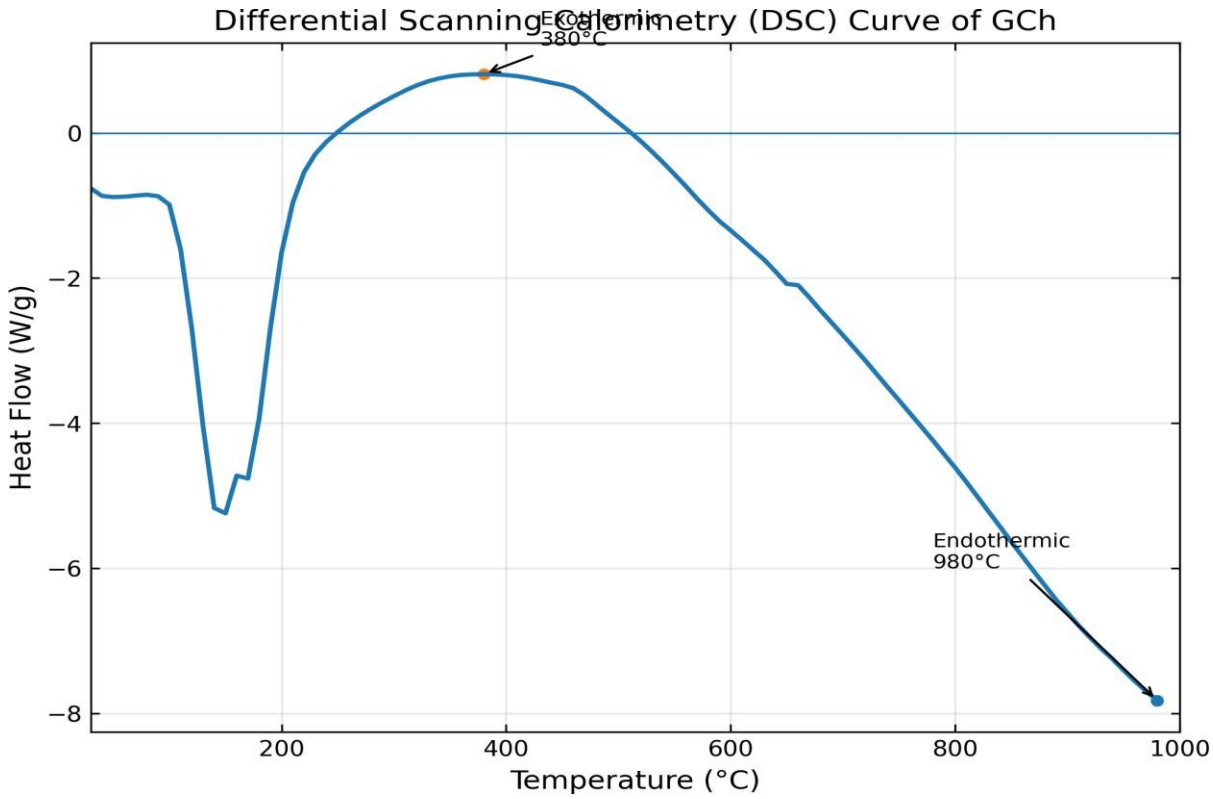

Fig.6: DSC curve (Heat Flow vs Temperature)

Summary of TGA Results

Stage	Temperature (°C)	Weight Loss (%)	Thermal Event
I	30–100	1.22	Moisture removal
II	100–180	33.79	Major decomposition
III	180–350	6.54	Carbonization and degradation
IV	350–600	1.49	Stable residue formation
V	600–980	4.63	Slow decomposition of residue
Total	30–980	47.67	Overall degradation

4.6 RAMAN ANALYSIS

Raman spectroscopy was employed to investigate the vibrational characteristics and structural ordering of the synthesized sample. The recorded spectrum covers the range of approximately 28–3894 cm^{-1} and exhibits a well-defined Raman profile with a prominent Raman band centered around 1390-1420 cm^{-1}, indicating strong vibrational activity associated with the material's crystal lattice corresponding to the stretching vibration of B–O bonds in borate structural groups [17]. This further confirms the formation of the borate glass network.

The Raman spectrum confirms the successful formation of the synthesized material with a distinct and intense Raman band near 1393 cm^{-1}. The well-defined spectral profile and absence of significant extraneous peaks indicate good structural quality and phase purity. Overall, the Raman results support the structural integrity of the synthesized Nd^{3+}-doped B_2O_3–LiF glass and complement other characterization techniques such as XRD, FTIR, FESEM, and TEM for comprehensive materials analysis.

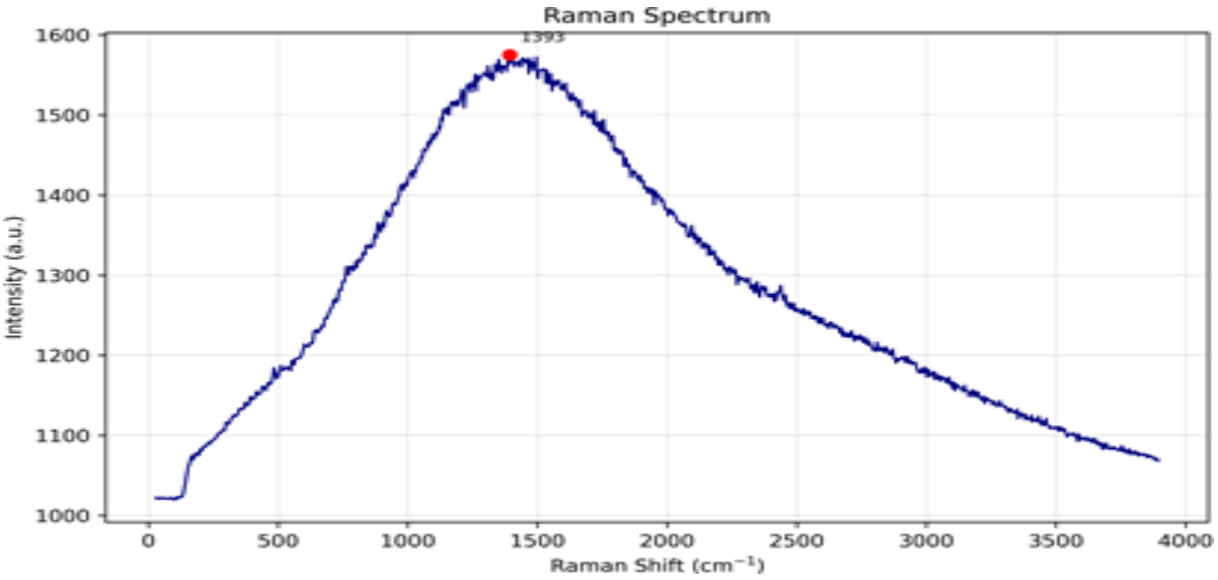

Fig.7: Raman spectrum of the synthesized Nd^{3+} B_2O_3-LiF glass

4.7 DIELECTRIC PROPERTIES

The plot frequency versus series capacitance shows that the series capacitance remains nearly constant at 76.6 pF at 5 kHz. Cs gradually decreases with increasing frequency. Between 5 kHz and 10 MHz, the capacitance changes only slightly from 76.6 pF to about 56 pF, indicating stable dielectric behaviour and confirms that the dielectric material possesses good polarization stability. The gradual reduction in capacitance with increasing frequency occurs because dipoles cannot respond completely to the rapidly varying electric field. Beyond 12 MHz, the capacitance decreases rapidly. At 25.142 MHz, Cs becomes negative (-68.648 pF). At 30.027 MHz, Cs reaches −276.57 pF, indicating resonance inductive effects.

255DDGD

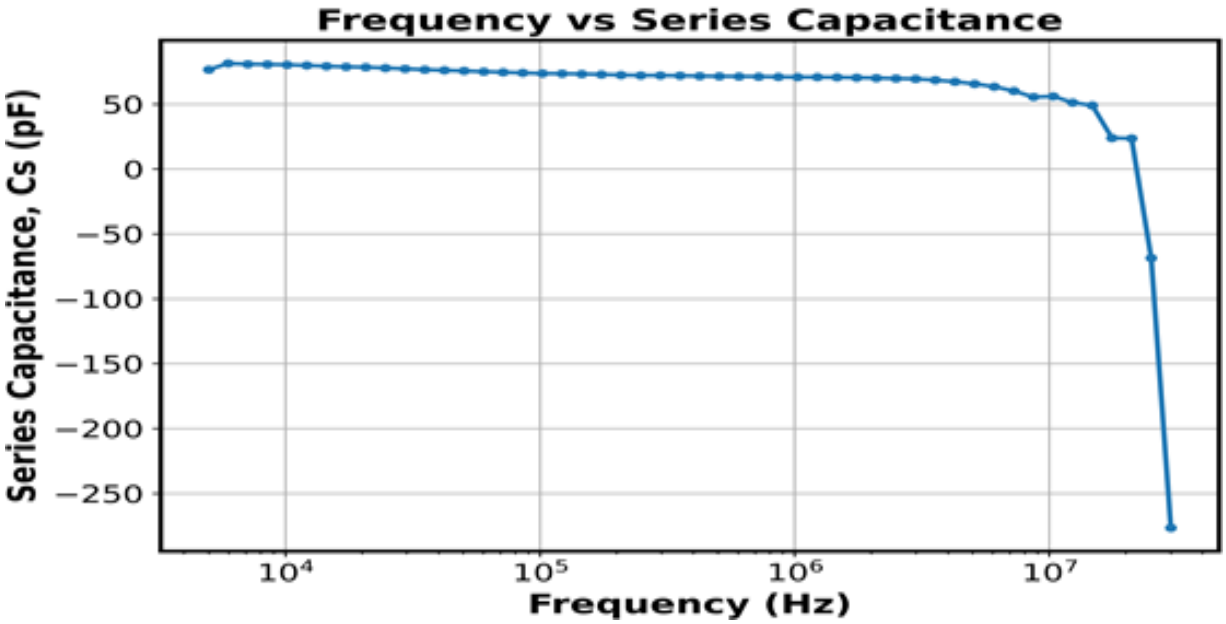

Fig.8: Plot of Frequency versus Series Capacitance of Nd^{3+}:B_2O_3-LiF glass

Frequency Dependence dissipation Factor

Frequency Dependence of tan δ shows that tan δ value decreases with increasing frequency indicates reduced dielectric losses and improved energy storage capability. The sudden increase beyond approximately 17 MHz is attributed to dielectric relaxation and resonance effects. The large tan δ near 25 MHz signifies strong energy dissipation caused by parasitic impedance and resonance.

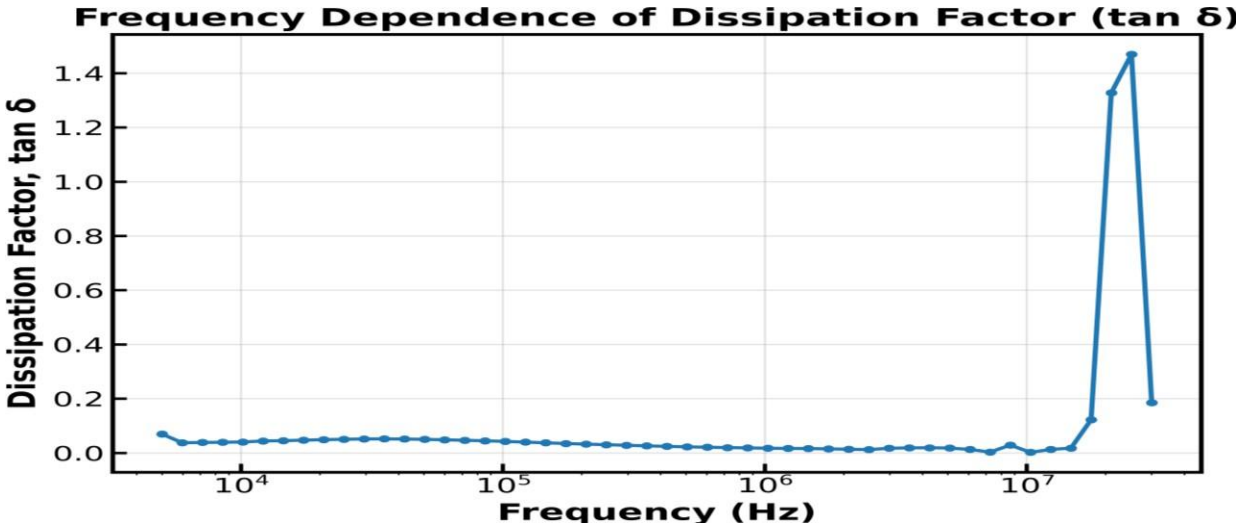

Fig.9: Frequency Dependence of Dissipation Factor (tan δ)

Frequency Dependence of Quality Factor (Q)

- Q increases steadily from 14.4 at 5 kHz.
- Maximum Q = 487.6 at 10.347 MHz.
- Q falls sharply after resonance.

A higher Q factor indicates lower dielectric losses and better capacitor performance. The peak near 10 MHz corresponds to the optimum operating frequency. Beyond resonance, dielectric losses dominate, causing Q to decrease rapidly.

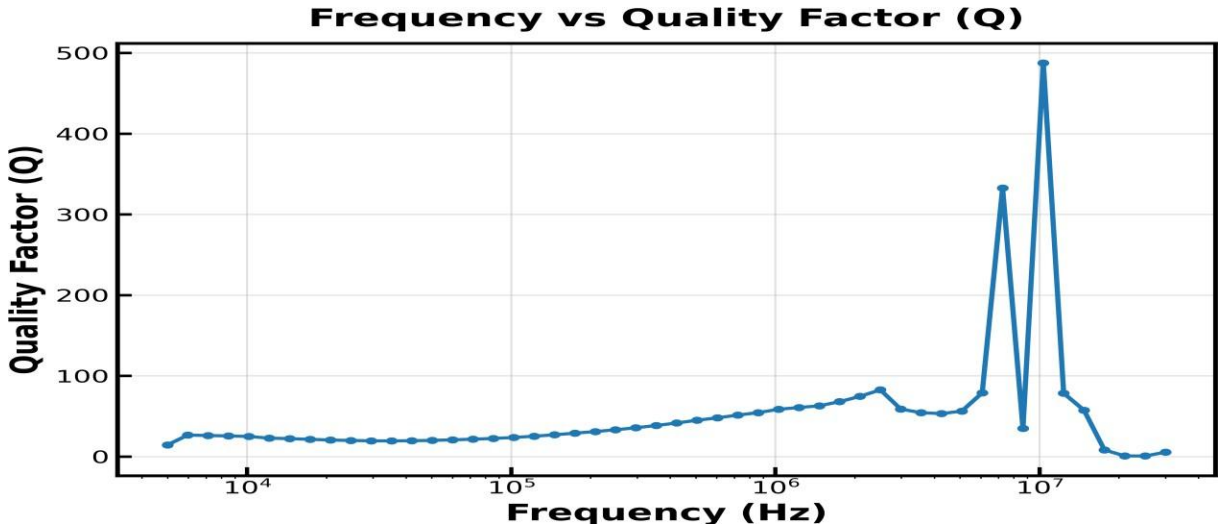

Fig.10: Plot of Frequency versus Quality Factor of Nd^{3+}:B_2O_3-LiF glass

Frequency Dependence of Impedance

Impedance decreases from 416.5 kΩ at 5 kHz to 19.5 Ω at 30 MHz. This behaviour is characteristic of capacitive materials because capacitive reactance decreases with increasing frequency[18].

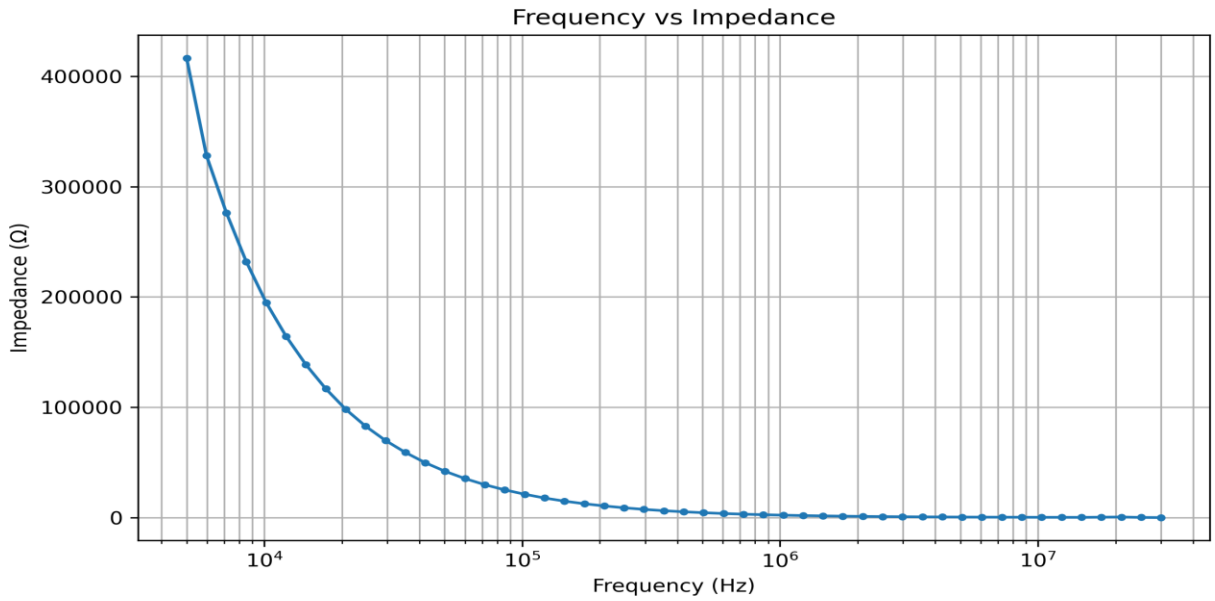

Fig.11: Plot of Frequency versus Impedance of Nd^{3+}:B_2O_3-LiF glass

Overall Results

Parameter	Observation
Series Capacitance	Nearly constant up to ~10 MHz, then decreases rapidly
tan δ	Decreases initially, minimum near 10 MHz, rises sharply after resonance
Quality Factor	Maximum (~488) near 10.3 MHz
Impedance	Decreases continuously with frequency
Phase Angle	Close to −90° before resonance, changes rapidly after resonance
Resonance Region	Approximately 20–30 MHz

The dielectric material exhibits excellent capacitive stability and low dielectric loss over a broad frequency range up to approximately 10 MHz. The highest quality factor and minimum dissipation factor indicate the optimum operating region around 10 MHz. Above 20 MHz, resonance and parasitic inductive effects become dominant, causing negative capacitance, increased dielectric loss, and rapid phase changes. Therefore, the material is well suited for high-frequency capacitor and electronic applications below the resonance frequency, where stable dielectric performance is maintained.

The dielectric constant decreased with increasing frequency due to dielectric dispersion. The dielectric loss showed relaxation behaviour, while AC conductivity increased with frequency because of enhanced charge carrier hopping within the glass matrix. These electrical characteristics indicate that Nd^{3+}-doped lithium borate glass possesses suitable dielectric behaviours for optoelectronic applications.

V. APPLICATIONS

The prepared Nd^{3+}-doped lithium borate glasses have significant potential in:

- Solid-state laser materials
- Optical fiber communication
- Optical amplifiers
- Near-infrared photonic devices
- Luminescent display systems
- Optical sensors
- Integrated photonic circuits

These applications arise from their excellent transparency, thermal stability, and efficient near-infrared luminescence.

VI. CONCLUSION

Transparent Nd^{3+}-doped lithium borate glasses were successfully synthesized using the conventional melt-quenching technique. Structural characterization confirmed the amorphous nature of the glass, while FTIR and Raman spectroscopy verified the borate network structure. Optical absorption and photoluminescence studies demonstrated characteristic Nd^{3+} transitions with strong near-infrared emission at 894, 1063, and 1330 nm. Thermal analysis indicated good thermal stability, and dielectric measurements revealed normal dielectric dispersion with increasing AC conductivity. Overall, the investigated glasses exhibit excellent structural, optical, thermal, and electrical properties, making them promising materials for advanced laser systems, optical amplifiers, fiber optics, and modern photonic technologies.

REFERENCES

[1] James F.A.J.L., Notes and Records R. Soc.London,38(1983)79-107

[2] E.Desurvire, Erbium-Doped Fiber Amplifiers,Principles and Applications, (John Wiley, Newyork) 1994.

[3] Digonnet M.J.F., Rare-Earth Doped Lasers and Fiber Amplifiers (Marcel Dekker, Inc.) 2001

[4] G.Fuxi, Optical and Spectroscopic Properties of Glass,Springer-Verlag, Berlin,1992

[5] B.R.Judd, Phys.Rev.127(1962)750.

[6] M.J.F.Digonnet, Marcel Dekker Rare Earth doped Fiber Laser and Amplifiers, New York,1993

[7] C. Gautam, A. K. Yadav, and A. K. Singh, "A Review on Infrared Spectroscopy of Borate Glasses with Effects of Different Additives," *ISRN Ceramics*, 2012, Article ID 428497

[8] B. N. Meera and J. Ramakrishna, "Raman spectral studies of borate glasses," *Journal of Non-Crystalline Solids*, 159 (1993) DOI: 10.1016/0022-3093(93)91277-A.

[9] M. A. Morsy, T. F. Garrison, M. R. Kessler, M. H. A. Mhareb, and H. Zahr El-Deen, "Structural Elucidation of Lithium Borate Glasses Using XRD, FTIR, and EPR Spectroscopy," *ACS Physical Chemistry* DOI: 10.1021/acsphyschemau.4c00106.

[10] Gautam, C.; Yadav, A. K.; Singh, A. K. A Review on Infrared Spectroscopy of Borate Glasses with Effects of Different Additives. *ISRN Ceramics* (2012) 428497. DOI: 10.5402/2012/428497

[11] Insiripong, S.; Kaewjeang, S.; Maghanemi, U.; Kim, H. J.; Chanthima, N.; Kaewkhao, J. NIR and upconversion luminescence properties of Nd^{3+} doped Gd_2O_3–CaO–SiO_2–B_2O_3 glass system. (Kyungpook National University(KNU))

[12] T. Som and B. Karmakar, J. Alloys. Comp.476 (2009) 383.

[13] H. Suna, L. Zhanga, M. Liaoa, G. Zhoua, C. Yua, J. Zhanga, L. Hua and Z. Jiang, J. Lumin.117 (2006) 179.

[14] W. A Pisarski, J. Pisarska , R. Lisiecki , L. Grobelny, G. Dominiak-Dzik and W. R. Romanowski, Chem.Phys.Lett.472 (2009) 217.

[15] A. A. Mekki et al./related borate glass thermal-stability literature using Tg, Tx and DSC/DTA criteria.

[16] M. A. Morsy et al., "Structural Elucidation of Lithium Borate Glasses Using XRD, FTIR, and EPR Spectroscopy," *ACS Physical Chemistry Au*, 5 (2025) 227–238

[17] C. S. Pavan Kumar, S. Pratap, C. S. Sumuka, and N. Sivasankara Reddy, "Review on the structure of borate glasses by Raman spectroscopic technique," *Ceramics International*, 52 (2026) 1359–1382

[18] A. S. Nowick and B. S. Lim, "Analysis of ac conductivity data for $Na_2O{\cdot}3SiO_2$ glass by stretched exponential and Jonscher power-law methods," *Journal of Non-Crystalline Solids*, 172–174 (1994) 1389–1394